ChemPubSoc Europe

DOI: 10.1002/chem.201601809

CHEMISTRY
A European Journal
Full Paper

Drug Discovery

Ferrocenyl Paclitaxel and Docetaxel Derivatives: Impact of an Organometallic Moiety on the Mode of Action of Taxanes

Anna Wieczorek,[a] Andrzej Błauż,[b] Aleksandra Żal,[b] Homayon John Arabshahi,[c] Jóhannes Reynisson,[c] Christian G. Hartinger,[c] Błażej Rychlik,*[b] and Damian Plażuk*[a]

Abstract: A series of ferrocenyl analogues and derivatives of paclitaxel and docetaxel were synthesised and assayed for their antiproliferative/cytotoxic effects, impact on the cell cycle distribution and ability to induce tubulin polymerisation. The replacement of the 3′-*N*-benzoyl group of paclitaxel with a ferrocenoyl moiety, in particular, led to formation of an analogue that was at least one order of magnitude more potent in terms of antiproliferative activity than the parent compound (IC_{50} values of 0.11 versus 1.11 μM, respectively), but still preserved the classical taxane mode of action, that is, microtubule stabilisation leading to mitotic arrest. Molecular docking studies revealed an unexpected binding pocket in the tubulin structure for the ferrocenoyl group introduced in the paclitaxel backbone.

Introduction

The antineoplastic agent paclitaxel (Taxol)[1] **1** promotes polymerisation of tubulin and stabilises microtubules, thus disturbing cellular division and, consequently, leading to cell death.[2,3] It was approved by the FDA for treatment of advanced ovarian and breast cancer in 1992. Since that time, paclitaxel and its semisynthetic analogue docetaxel **2**, which was approved by the FDA in 1994, are widely used chemotherapeutics for treatment of many types of neoplastic diseases, including, but not limited to lung, ovarian, breast, head and neck cancers, melanoma and Kaposi's sarcoma (Figure 1).[4,5]

In the last two decades, a large number of structure–activity relationship (SAR) studies of modified paclitaxel have been published.[6] Two main types of structural modifications of **1** were carried out: modifications performed at the side chain of paclitaxel and at the taxol skeleton. Usually, the modification of the paclitaxel side chain strongly affects its antiproliferative activity, in some cases increasing the anticancer activity in comparison to paclitaxel[6a,f,j] (e.g., esterification of the 2′-hydroxy group with polyunsaturated fatty acids increases its activity against drug-resistant colon and drug-sensitive ovarian tumours in mice,[17] and replacement of the 3′-phenyl group by alkyl, alkenyl or aryl groups or modification of 3′-*N*-acyl group also improves cytotoxicity[7,8]). On the other hand, the influence of modifying the paclitaxel skeleton on its cytotoxicity strongly depends on the modification site, for example, acylation or epimerisation of the 7-OH group usually do not influence or even lead to a lack of activity of the resulting compound, whereas modification of the 3-benzoyloxy group usually improves cytotoxicity.[9]

The success of platinum-based complexes, such as cisplatin, in anticancer therapy stimulated to search for new metal-containing anticancer drug candidates. Tremendous progress in bioorganometallic chemistry has led to the development of anticancer,[10] antimalarial[10a,11] and antibacterial[12] compounds in

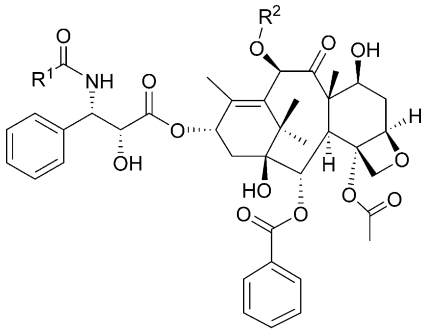

1 R^1=Ph, R^2=Ac
2 R^1=*t*BuO, R^2=H

Figure 1. The structures of paclitaxel **1** and docetaxel **2**.

[a] *A. Wieczorek, Dr. D. Plażuk*
Department of Organic Chemistry
Faculty of Chemistry
University of Łódź
Tamka 12, 41-403 Łódź (Poland)
E-mail: damplaz@uni.lodz.pl

[b] *Dr. A. Błauż, A. Żal, Dr. B. Rychlik*
Cytometry Lab
Department of Molecular Biophysics
Faculty of Biology and Environmental Protection
University of Łódź
ul. Pomorska 141/143, 90-236 Łódź (Poland)
E-mail: brychlik@biol.uni.lodz.pl

[c] *H. J. Arabshahi, Dr. J. Reynisson, Prof. Dr. C. G. Hartinger*
School of Chemical Sciences
The University of Auckland
Private Bag 92019, Auckland 1142 (New Zealand)

Supporting information and the ORCID identification number(s) for the author(s) of this article can be found under http://dx.doi.org/10.1002/chem.201601809.

recent years. A metal atom in various oxidation states gives access to structural diversity and biological properties that are different from those of typical organic compounds.[14] Depending on the nature of the metal–ligand bond, bioactive organometallic compounds may feature covalent metal–carbon bonds and/or labile ligands. Ferrocene is a redox active metallocene that is non-cytotoxic and stable in biological media. However, when incorporated in or conjugated with biologically active compounds, it provides access to promising cytotoxic agents with non-conventional modes of action. Many ferrocenyl compounds have recently been prepared through conjugation of a ferrocene moiety with nucleobases,[13] peptides, vitamins[14] or phenols,[15] which exhibited significant anticancer,[16] antimalarial[11a,17] or antibacterial[18] activity. Some of these compounds exhibited unexpected novel properties, for example, ferrocenyl curcuminoids interfered with microtubule polymerisation.[19]

In our continuous efforts to develop organometallic anticancer agents, we developed and studied the biological properties of ferrocenyl-functionalised taxanes, such as paclitaxel and docetaxel, which are low-molecular mass microtubule depolymerisation inhibitors, as new antimitotic drug candidates. Our preliminary study showed that a simple esterification of paclitaxel with ferrocenecarboxylic acid and 3-ferrocenoylpropionic acid at the 2′-*O*-position leads to highly cytotoxic ferrocenyl conjugates.[20] Thus, we decided to investigate in a more detailed way the mode of action of ferrocenyl-modified taxanes focusing on their interference with the cellular microtubule network. We prepared two sets of ferrocenyl analogues and conjugates of paclitaxel and docetaxel having the organometallic group at the side chain of paclitaxel and at the taxol skeleton. In particular, we describe the synthesis and studies of the interaction with tubulin, the impact on the cell cycle distribution and the cytotoxic activity. As several ferrocenyl derivatives show increased activity against multidrug resistant cells (e.g., a ferrocenyl plinabulin analogue)[21] the antiproliferative activity of the organometallic taxanes in cells exhibiting elevated expression of specific ABC transporters responsible for the MDR (multidrug resistance) phenotype were also assayed.

Results and Discussion

To synthesise ferrocenyl analogues of paclitaxel bearing a ferrocenoyl group instead of the benzoyl group at the 3′-*N* position, an established procedure was adopted,[22] starting from optically pure (*3R,4S*)-3-triethylsilyloxy-4-phenylazetidin-2-one (**5**) and 10-deacetylbaccatin III (**3**). In the reaction of **3** with triethylsilylchloride (TESCl) in pyridine,[23] the 7-OH group was selectively protected as a triethylsilyl ether, followed by a selective *O*-acetylation of the 10-OH with LiHMDS and acetyl chloride in THF at −40 °C for 30 min leading to the desired compound **4** in 85% overall yield (Scheme 1). Introduction of the (*3R,4S*)-phenylisoserine moiety at the 13-OH position of **4** required the use of optically pure *N*-ferroceneazetidin-2-ones. (*3R,4S*)-*N*-Ferrocenoyl-4-phenyl-3-triethylsilyloxyazetidin-2-one (**6**) was prepared in 52% yield in an *N*-acylation reaction of **5** with freshly prepared ferrocenoyl chloride (prepared from ferrocenecarboxylic acid and slight excess of oxalyl chloride at RT[24]). The *N*-acylation of **5** with 4-ferrocenebutyric acid using an excess of diisopropylcarbodiimide (DIC) as a coupling agent in the presence of a catalytic amount of 4-dimethylaminopyridine (DMAP) in dichloromethane at RT led to *N*-(4-*f*errocenylbutyryl)-3-triethylsilyloxyazetidin-2-one (**7**) in 56% yield (Scheme 2).

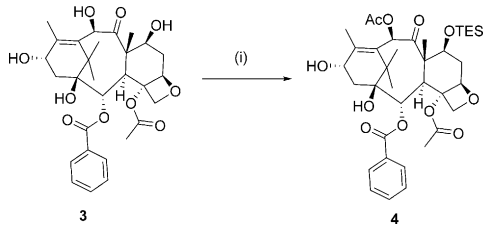

Scheme 1. Synthesis of compound **4**. Reagents and conditions: (i) (a) TESCl, pyridine, RT, 5 min; (b) LiHMDS, then CH_3COCl, THF, −40 °C, 30 min.

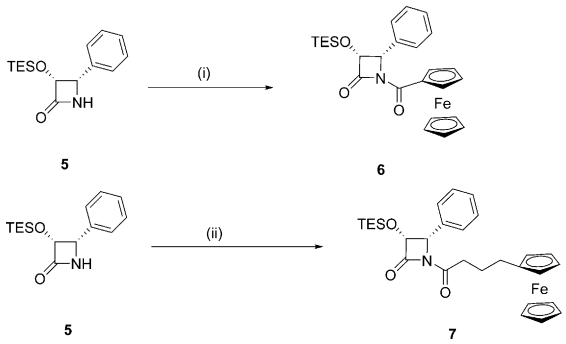

Scheme 2. Synthesis of N-ferrocenyl-substituted azetidin-2-ones **6** and **7**. Reagents and conditions: (i) FcCOCl (Fc = ferrocenyl), Et_3N, DMAP, DCM, 0–RT, 2 h; (ii) $Fc(CH_2)_3COOH$, DIC, DMAP, DCM, RT, 24 h.

In the next step, 13-*O*-acylation of **4** with azetidin-2-ones **6** and **7** under typical conditions[22a] using LiHMDS as a base at −40 °C gave the corresponding paclitaxels **8** and **9** in good yields of up to 84%. Further deprotection of hydroxy groups with an excess of HF·pyridine (HF·Py) in a solution of pyridine and acetonitrile at RT for 24 h gave the desired ferrocenyl analogues of paclitaxel **10** and **11** in good yields of up to 90% (Scheme 3).

To introduce a ferrocenyl moiety at the 2′-*O*-position of paclitaxel and docetaxel, an established procedure was used for selective acylation of **1** and **2** with various ferrocenecarboxylic acids (Scheme 4).[20] The desired 2′-*O*-ferrocenyl substituted paclitaxels **12**–**15** and docetaxel derivatives **16**–**19** were obtained in good to excellent yields.

Paclitaxel and docetaxel conjugates bearing a ferrocenyl substituent at the 7-*O*-position were synthesised in three steps, starting from **1** and **2** (Scheme 5). In the first step, **1** and **2** were selectively protected at the 2′-*O*-position as *tert*-butyldimethylsilyl ethers with *tert*-butyldimethylsilyl chloride (TBSCl) in the presence of imidazole in DMF at RT.[25]

The resulting 2′-*O*-TBS-paclitaxel **20** was then selectively 7-*O*-acylated with 3-ferrocenoylpropionic acid or 4-ferrocenylbuty-

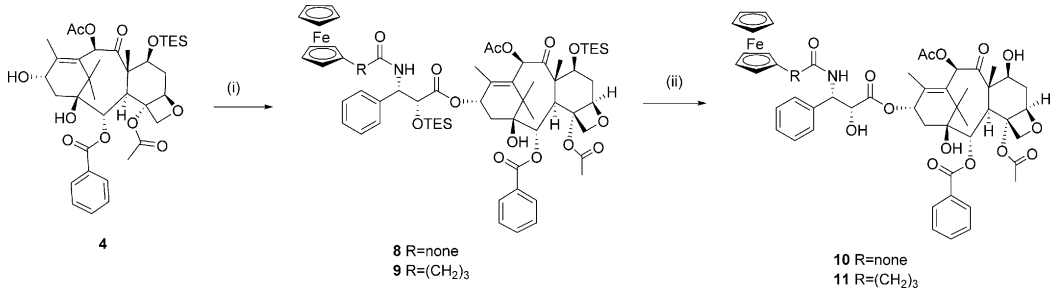

Scheme 3. Synthesis of *N*-debenzoyl-*N*-ferrocenoylpaclitaxel derivatives **10** and **11**. Reagents and conditions: (i) **6** or **7**, LiHMDS, THF, −40 °C, 40 min, up to 84% yield; (ii) HF·Py, pyridine/MeCN, RT, 24 h, up to 90% yield.

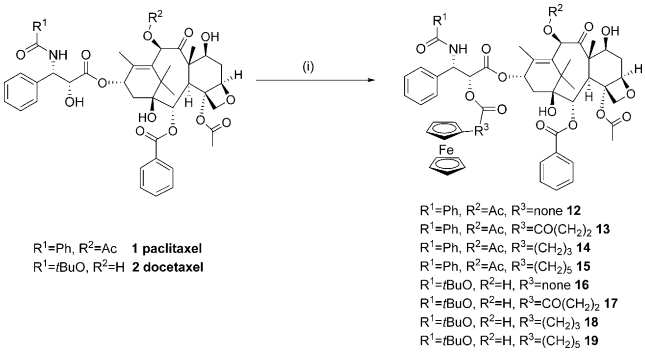

Scheme 4. Synthesis of 2′-O-ferrocene-substituted paclitaxel **12**–**15** and docetaxel **16**–**19** derivatives. Reagents and conditions: (i) FcR^3COOH, DIC (1.5 equiv), DMAP (0.1 equiv), DCM, RT, 24 h.

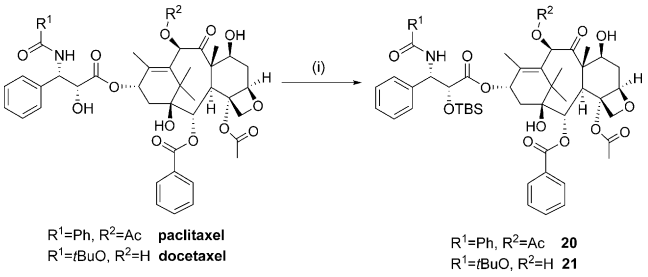

Scheme 5. Synthesis of 2′-O-TBS ethers of paclitaxel **20** and docetaxel **21**. Reagents and conditions: (i) TBSCl, imidazole, RT, 24 h.

ric acid using DIC as a coupling agent at 0 °C, whereas attempts to use ferrocenecarboxylic acid as an acylation agent under various conditions failed. The corresponding products **22** and **23**, respectively, were isolated in good or excellent yields by chromatography on silica column (Scheme 6). A similar reaction of 2′-*O*-TBS-docetaxel **21** with 5-ferrocenoylpentanoic and 6-ferrocenylhexanoic acids as acylating agents carried out at 0 °C gave the desired 7-*O*-acylated-2′-*O*-TBS-docetaxel derivatives **24** and **25**, respectively, as major products. In this reaction, small amounts of 10-*O*-isomers were also formed (less than 5%). The deprotection of hydroxy groups in **22**–**25**, carried out using HF·Py, gave the desired 7-*O*-ferrocenyl-substituted taxanes **26**–**29**, respectively, in good to excellent yields (Scheme 7).

Cytotoxic activity

SW620 cells originating from human colon adenocarcinoma were chosen to screen the synthesised ferrocenyl taxanes for their in vitro antiproliferative/cytotoxic activity in comparison to **1** and **2**. The SW620 cell line is characterised by a relatively high sensitivity towards various chemotherapeutics as established by cytotoxicity assays,[26] thus being well-suited for studying the activity of novel compounds of an uncertain mechanism of action. To investigate whether ferrocenyl taxanes are able to overcome multidrug resistance (MDR) resulting from overexpression of various ABC proteins, we further employed a panel of five SW620-derived drug resistant cancer cell lines (SW620C, D, E, M and V) obtained by a stepwise selection with the classical anticancer agents cisplatin, doxorubicin, etoposide, methotrexate and vincristine, respectively.[20,21] The MDR cell lines were fully characterised with regards to drug cross-resistance, ABC transporter protein expression and the subcellular localisation and activity of the drugs. These cell

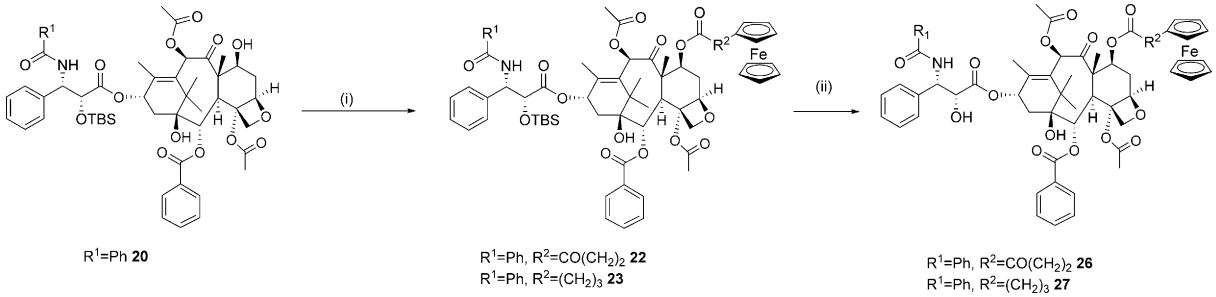

Scheme 6. Synthesis of paclitaxel derivatives **26** and **27** substituted in the 7-position with a ferrocene moiety. Reagents and conditions: (i) FcR^2COOH, DIC (1.5 equiv), DMAP (0.1 equiv), DCM, RT, 24 h; (ii) HF·Py/pyridine/MeCN, RT, 24 h.

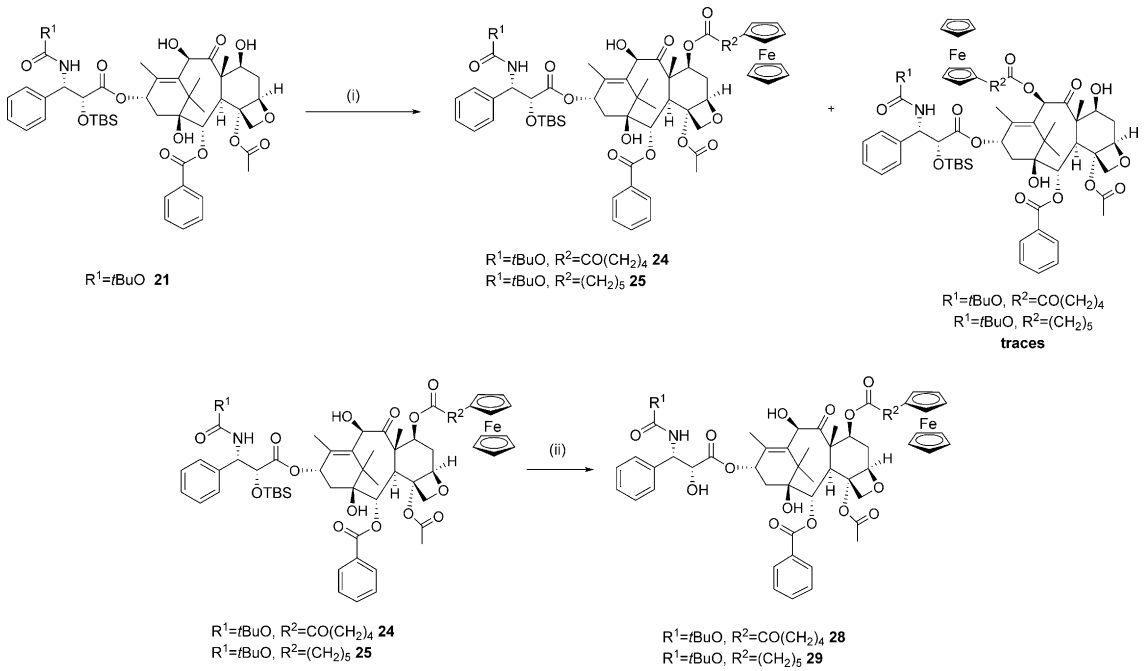

Scheme 7. Synthesis of docetaxel derivatives **28** and **29** substituted in the 7-position with ferrocene. Reagents and conditions: (i) FcR^2COOH, DIC (1.5 equiv), DMAP (0.1 equiv), DCM, RT, 24 h; (ii) HF·Py/pyridine/MeCN, RT, 24 h.

lines are ranked in the following order with regard to the expression of the ABC transporter ABCB1 (either at mRNA or protein level): SW620V > SW620D > SW620E ≫ SW620C > SW620M = SW620. ABCB1 was recognised as a high contributor to taxane resistance.[27] The IC_{50} values and corresponding 95%-confidence intervals for all of the synthesised compounds are summarised in Table 1. All compounds were analysed at a concentration range between 3 nM and 30 μM, whereas higher concentrations are unlikely to be obtained in any bodily fluid in vivo (peak paclitaxel serum concentration achievable after parenteral administration of a maximum allowable dose is only 4.5 μM).[28]

All compounds demonstrated antiproliferative/cytotoxic action against the parental cell line SW620 in the micromolar or even submicromolar concentration range. It is noteworthy that the simplest ferrocenyl analogue of taxol (**10**) obtained by replacing the *N*-benzoyl group with a ferrocenoyl moiety, exerted increased antiproliferative/cytotoxic effects compared to paclitaxel (IC_{50} value of 0.11 vs 1.11 μM for **10** and **1**, respectively). Insertion of a butyryl spacer between the ferrocenyl moiety and the amine group, as in **11**, results in a four-fold alleviation of the cytotoxic activity. The cytotoxicity of compounds bearing a ferrocenyl moiety attached to the 2′-OH group of paclitaxel (**12**–**15**) strongly depends on the linker type. Compound **13** is as active as paclitaxel against SW620 cells (IC_{50} = 0.84 μM), but its activity is lower than that of **10**. All other compounds of this series (**12**, **14** and **15**) are markedly (two–ten times, taking into account the mean values) less active than paclitaxel **1**. Additionally, the presence of a ferrocenyl moiety attached to the 7-OH group, further decreases the antiproliferative activity of the synthesised compounds compared to **1**. All synthesised derivatives of docetaxel (**16**–**19** and **28**–**29**) exhibit approximately one order of magnitude lower activity than the parent compound, except for **28**, which is only 2.7 times less active.

When analysing the response of drug resistant cells to the new compounds, it is clear that none of them are potent enough to overcome the MDR barrier. All substances were active against SW620M cells, which is not surprising, as they do not overexpress ABCB1 compared to the parental cell line. However, the IC_{50} values determined for this cell line were on average four–five times higher than those for SW620 cells (except for **10** and **28**, for which they were 60 and 110 times higher, respectively). It may suggest an impact of ABCC1, which is a highly overexpressed ABC transporter in SW620M cells[29] in conferring low-level resistance to the analysed taxanes. It should also be mentioned that the paclitaxel derivatives **11** and **27** exhibited activity against SW620C cells (expressing ABCG2), whereas only **18** of the ferrocenyl derivatives of the docetaxel series exerted a moderate cytotoxic activity against SW620E (expressing both ABCB1 and ABCC1).

It is interesting to compare the viability of SW620 cells in the presence of different concentrations of the synthesised compounds. The viability of SW620 cells at 10 nM concentration of **10** is as low as 61% (Figure S1 in the Supporting Information), whereas all other compounds are slightly, if at all, active at this concentration. At 100 nM, the simplest ferrocenyl analogue of paclitaxel **10** was still the most active derivative but also **1**, **2** and **28** showed some activity (41% viability compared to 64, 60 and 63%, respectively). At 1 μM, only two of the synthesised compounds (**14** and **27**, both from the paclitaxel series) did not significantly affect the viability of the SW620 cells (84 and 102%, respectively).

Table 1. Cytotoxicity of the ferrocenyl compounds **10**–**19** and **26**–**29** in reference to paclitaxel **1** and docetaxel **2** as determined by the MTT-reduction viability assay (MTT = 3-(4,5-dimethylthiazol-2-yl)-2,5-diphenyltetrazolium bromide).[a]

Compound	IC_{50} [μM] SW620	SW620C	SW620M
1	1.11 [0.46–1.49]	N.D.	6.72 [4.26–10.60]
10	0.11 [0.07–0.19]	N.D.	6.65 [2.97–14.86]
11	5.18 [3.38–7.94]	45.26 [25.8–79.39]	7.83 [4.84–12.67]
12	7.88 [5.33–11.66]	N.D.	21.32 [14.63–31.07]
13	0.84 [0.69–1.02]	N.D.	3.36 [2.48–4.53]
14	12.71 [10.33–15.62]	N.D.	29.55 [18.05–48.39]
15	2.53 [2.00–3.21]	N.D.	13.09 [8.63–19.87]
26	4.42 [3.76–5.19]	N.D.	19.74 [14.11–27.62]
27	6.91 [5.80–8.23]	N.D.	22.47 [14.05–35.92]
2	0.31 [0.22–0.43]	N.D.	1.49 [1.02–2.19]
16	1.47 [1.11–1.95]	N.D.	6.73 [4.16–11.49]
17	3.22 [1.92–5.40]	N.D.	7.16 [4.74–10.80]
18	2.30 [1.87–3.56]	N.D.	21.18 [10.36–42.04]
19	1.99 [1.79–3.07]	N.D.	26.48 [19.07–36.77]
28	0.83 [0.60–1.15]	N.D.	91.38 [32.61–256.1]
29	4.27 [3.36–6.58]	N.D.	23.05 [15.39–33.18]

[a] 95%-confidence intervals are given in brackets (please note that due to the log-transformation of the data required to perform IC_{50} calculations, these are asymmetrical). Calculations are based on results of three independent experiments. N.D. denotes situations in which the character of the viability data, due to low cytotoxicity, did not allow for proper curve fitting and IC_{50} calculation. This also applies to data for cell lines SW620D, SW620E, and SW620V

Table 2. Influence of the synthesised compounds on the cell cycle distribution of SW620 cells at 10 nM concentration.[a]

Compound	Cell cycle phase distribution [%] sub-G0/G1	G0/G1	S	G2/M
control[b]	1.6 ± 0.1	42.7 ± 3.5	47.7 ± 2.6	8.0 ± 0.9
DMSO[c]	1.6 ± 0.5	42.3 ± 5.5	47.9 ± 3.8	8.0 ± 2.4
1	21.8 ± 5.9	33.6 ± 3.5	40.1 ± 2.4	7.5 ± 5.4
10	41.0 ± 12.3	17.7 ± 7.4	31.5 ± 3.2	13.5 ± 2.6
11	5.1 ± 1.4	41.9 ± 5.3	44.9 ± 4.4	8.5 ± 2.3
12	2.6 ± 1.3	41.7 ± 4.0	46.9 ± 1.3	8.7 ± 1.1
13	18.1 ± 14.7	32.3 ± 9.8	41.7 ± 4.0	10.2 ± 0.2
14	2.7 ± 1.9	48.4 ± 4.5	42.3 ± 1.2	9.7 ± 1.4
15	3.2 ± 0.8	42.6 ± 2.6	45.9 ± 2.3	8.8 ± 2.8
26	3.0 ± 0.3	43.2 ± 5.9	46.7 ± 5.3	7.1 ± 0.8
27	2.2 ± 0.8	43.8 ± 6.8	45.6 ± 5.8	8.6 ± 0.7
2	38.3 ± 4.5	5.0 ± 4.0	19.2 ± 3.8	36.8 ± 3.2
16	11.3 ± 2.0	37.3 ± 1.8	44.2 ± 0.8	9.9 ± 4.2
17	33.1 ± 23.1	19.7 ± 15.2	28.1 ± 6.8	23.4 ± 8.0
18	7.2 ± 6.0	45.7 ± 4.2	40.1 ± 5.7	10.3 ± 5.0
19	7.8 ± 8.1	43.1 ± 3.0	42.3 ± 5.8	10.4 ± 4.6
28	7.8 ± 5.5	38.4 ± 1.2	45.8 ± 4.6	9.8 ± 2.2
29	4.0 ± 4.5	44.6 ± 2.5	43.9 ± 3.0	9.1 ± 1.9

[a] Averaged data ± SD calculated from three independent experiments. Cell cycle fractions were calculated by FlowJo software using Watson pragmatic algorithm. [b] Cells in a complete medium. [c] Cells in a complete medium supplemented with DMSO at the concentration used for investigated compounds.

Cell cycle distribution studies

The taxane-induced inability to rearrange microtubules prevents mitosis and results in cell death executed mainly through the mitotic catastrophe. Thus, taxane treatment significantly alters the cell cycle and leads to accumulation of G2/M cells (due to mitotic arrest) and increase in sub-G0/G1 fraction indicative of DNA fragmentation. Results of the SW620 cell cycle analysis following 48-hour incubation with the ferrocenyl taxane analogues at 10 nM are presented in Table 2.

Surprisingly, significant mitotic arrest, as indicated by elevated G2/M levels, was only found for **10**, **13** and **17**. It was accompanied by a high number of cells undergoing cell death, as indicated by elevation of sub-G0/G1 fraction (from approx. 1.5% in control samples to over 40% in the case of **10**). The latter effect, although to a lesser extent, was also observed for **11** and **16** (5.1% and 11.3%, respectively). In general, under the experimental conditions applied (48-hour exposure), paclitaxel **1** and its ferrocenyl analogues turned out to be potent inducers of apoptosis rather than of mitotic arrest, with **10** being again the most effective. On the other hand, both docetaxel and **17** induced cell death, as manifested by an abundant sub-G0/G1 fraction and G2/M blockage, which was inferred from alterations of specific cell cycle phases (at least half reduction of G0/G1 and S phase cell number, and simultaneous two–three fold increase in the G2/M phase fraction).

Tubulin polymerisation assay

The basis for microtubule stabilisation is a direct interaction of taxane and β-tubulin molecules, thus leading to microtubule stabilisation and prevention of their rearrangement. To check whether ferrocenyl derivatives are able to induce tubulin polymerisation, a fluorescence real-time assay was applied. As shown in Figure 2, the paclitaxel analogues **10** and **11** promote tubulin polymerisation much more efficiently than their parent compound **1**. Compound **26** induces tubulin polymerisation to a lesser extent than paclitaxel but still faster than DMSO, which was used as the solvent control. All other ferrocenyl derivatives of paclitaxel, that is, **12**–**15** and **27**, tend to decrease the tubulin polymerisation rate. When analysing the docetaxel series (Figure S2 in the Supporting Information), all derivatives are much weaker inducers of tubulin polymerisation than **2**. The most active of this series is **28**, which turned out to be as effective as paclitaxel. On the other hand, **18** was the only docetaxel analogue, which seemed to be an inhibitor of tubulin polymerisation.

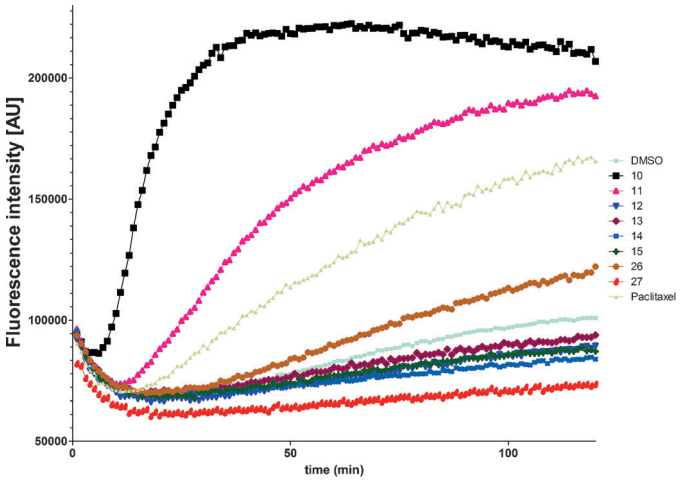

Figure 2. Tubulin polymerisation induced by ferrocenyl analogues of paclitaxel at 1 μM concentration. Results of a representative study from of a series of three independent experiments is presented.

The influence of the synthesised compounds on tubulin polymerisation and microtubule stabilisation was also investigated for SW620 cells using confocal microscopy. The results obtained for the most active compounds **10**, **11** and **13** compared to paclitaxel and vincristine as positive and negative controls, respectively, are summarised in Figure 3. Paclitaxel induces formation of microtubule bundles, which can be easily recognised in Figure 3b, whereas vincristine prevents tubulin dimer polymerisation, which results in uniform distribution of tubulin within the cytoplasm (Figure 3c). Cell treatment with both **10** and **11** significantly intensifies tubulin staining, visualised as a dense microtubule network (Figures 3d and 3e), although paclitaxel-specific microtubule bundles are seen only in the case of **13** (Figure 3f).

Docking studies with tubulin

To explain the findings from cytotoxicity assays and tubulin polymerisation assays and to estimate the likelihood of binding to tubulin, docking studies of tubulin (PDB: 1JFF) with the

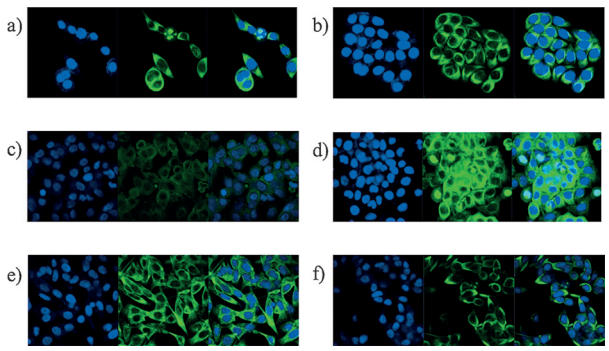

Figure 3. Influence of the synthesised compounds on microtubule formation in SW620 cells: a) untreated cells, b) paclitaxel **1**, c) vincristine, d) **10**, e) **11**, f) **13**; left panel: nuclear staining with Hoechst 33342; middle panel: anti β-tubulin antibody staining; right panel: superposition of images from the left and middle panels.

most active ferrocenyl analogue **10** were conducted and compared to **1** and **2**. Gold score (GS)[30] was the only scoring function able to treat the metal complexes. GS gives arbitrary numbers with higher values predicting better binding.

Docking of paclitaxel **1** resulted in two predicted hydrogen-bonding interactions (Figure S4a in the Supporting Information) with Gly370 and Thr276 and the compound gave a GS of 68. The binding site has hydrophobic pockets that the 3′ and the benzoyl amide phenyl rings of the ligand are predicted to occupy (Figure S4b). In proximity to His229, the 3′ and the benzoyl amide phenyl rings fill the hydrophobic pockets, whereas the tetracyclic fragment sits partially above the surface of the protein.

When docetaxel **2** was docked, it did not fully overlap with the conformation of paclitaxel (GS = 67). A hydrogen bonding interaction with Thr276 is predicted (Figure S5a in the Supporting Information), which was also seen for **1**. Similar predicted poses of the compounds resulted in comparable protein ligand hydrophobic interactions with the phenyl group in the 3′ position directed into the pocket (Figure S5b).

The ferrocenyl analogue of paclitaxel **10** has a good fit in the binding pocket of **1**. With a GS of 69, the scoring of the compound was very similar to **1** and **2**. Despite the structural similarity to **1**, a different hydrogen bonding pattern was observed, that is, a hydrogen bond with His229 (see Figure 4 and

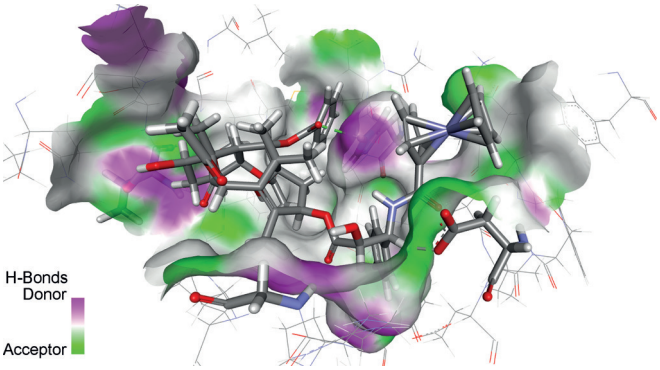

Figure 4. The docked configuration of **10** in the binding site of tubulin.

Figure S6a in the Supporting Information). The hydrophobic interactions are similar to paclitaxel. The 2-benzoyl side-chain phenyl and ferrocenyl moieties (Figure S6b) occupy the hydrophobic pockets. The similarity in docking between compound **10**, paclitaxel and docetaxel suggests a plausible binding to tubulin. Also, the hydrophobic interaction between the ferrocenyl moiety and the binding pocket supports this assumption. However, note that due to a small data set, it is difficult to draw ultimate conclusions.

Conclusions

A series of ferrocenyl derivatives of paclitaxel and docetaxel were synthesised and evaluated for both inducing tubulin polymerisation and their antiproliferative activity. The most potent compound, the simplest ferrocenyl analogue of pacli-

taxel **10**, was demonstrated to be more active toward SW620 cells and to induce tubulin polymerisation more efficiently than paclitaxel **1**. Compound **10** was able to induce apoptosis and arrest the cell cycle in the G2/M phase at least as effective as **1**. The high activity of **10** may be explained by its augmented interactions with β-tubulin as suggested by docking studies. Lower cytotoxic activity of **11** than that of **1**, together with its higher ability to induce polymerisation of tubulin to microtubules may suggest that the mechanism of action of **11** is different from that of paclitaxel and **10**. The tubulin polymerisation induced by this compound in a cellular system seems to be insufficient to exert its antiproliferative activity in a living cell. On the other hand, **13**, **15** and **16** appear to utilise mechanisms other than microtubule stabilisation for their cytotoxic/cytostatic activity.

Ferrocenyl analogues of taxanes are an interesting class of organometallic compounds. The bioactivity of the synthesised compounds described here demonstrates that the ferrocenyl moiety has a positive impact on the activity of a taxane as both an activator of tubulin polymerisation and an antiproliferative agent. The preliminary data on these organometallic compounds, which are able to induce or inhibit polymerisation of tubulin and act as anticancer drug candidates, warrants further investigation. Additionally, the exact mode of action of the most active ferrocenyl taxanes is currently unknown and requires further studies. Other ferrocene derivatives, for example, ferrocifen,[31] ferroquine[32] and ferrocenyl-based antifungal agents[33] are thought to act by producing reactive species through a Fenton-type reaction. Thus, the toxicity of ferrocene conjugates can be explained by the fact that an organic ligand acts as a trafficking agent to place ferrocene in the vicinity of a particular cellular target, where oxidation of the iron ion and production of hydroxyl and superoxide radicals induces damage. Further studies to explain the mechanism of cytotoxicity of ferrocenyl taxanes combining the measurement of redox potential and intracellular generation of reactive oxygen species (ROS) production, especially in comparison to ruthenocenyl derivatives, are planned and will be performed in the near future.

Experimental Section

(3*R*,4*S*)-1-Ferrocenoyl-4-phenyl-3-((triethylsilyl)oxy)azetidin-2-one (6): Oxalyl chloride (525 mg, 350 μL, 4.14 mmol) and 1 drop of DMF as catalyst were added to a slurry of ferrocenecarboxylic acid (506 mg, 2.2 mmol) in 10 mL of anhydrous dichloromethane. The resulting solution was stirred at RT for 1 h and the volatile materials were removed by evaporation. The crude ferrocenoyl chloride was dried prior to use for 30 min under vacuum (at 0.01 mbar). (3*R*,4*S*)-4-phenyl-3-((triethylsilyl)oxy)azetidin-2-one (**5**, 470 mg, 1.694 mmol), DMAP (200 mg, 1.637 mmol) and anhydrous triethylamine (607 mg, 836 μL, 6.0 mmol) in anhydrous DCM (5 mL) were placed in a Schlenk tube. A solution of freshly prepared ferrocenoyl chloride in anhydrous DCM (5 mL) was added dropwise at 0 °C and the resulting mixture was stirred at RT for 2 h. Then 50 mL of saturated sodium bicarbonate was added and the product was extracted with ethyl acetate. The organic phase was washed with brine, dried and the solvent removed. Chromatography on silica gel (300 mL of silica gel, *n*-hexane/ethyl acetate 4:1) gave pure **6** as a dark red oil (430 mg, 52%). ^{1}H NMR (600 MHz, $CDCl_3$): δ = 7.34–7.41 (m, 4H), 7.29–7.33 (m, 1H), 5.44–5.47 (m, 1H), 5.29 (d, J = 6.4 Hz, 1H), 5.17–5.20 (m, 1H), 5.08 (d, J = 6.0 Hz, 1H), 4.50–4.53 (m, 2H), 4.15 (s, 5H), 0.82 (t, J = 7.9 Hz, 9H), 0.43–0.56 ppm (m, 6H); ^{13}C{^{1}H} NMR (151 MHz, $CDCl_3$): δ = 169.4, 164.5, 134.4, 128.4, 128.3, 128.1, 75.2, 72.3, 72.3, 72.1, 71.8, 70.7, 70.0, 60.8, 6.3, 4.5 ppm; HRMS (EI) calculated for $C_{26}H_{31}FeNO_3Si$ 489.14176, found 489.14218.

(3*R*,4*S*)-1-(4-Ferrocenylbutyryl)-4-phenyl-3-((triethylsilyl)oxy)azetidin-2-one (**7**): DIC (91 mg, 112 μL, 0.721 mmol) was added to a solution of (3*R*,4*S*)-4-phenyl-3-((triethylsilyl)oxy)azetidin-2-one (**5**, 100 mg, 0.360 mmol), 4-ferrocenylbutyric acid (103 mg, 0.378 mmol), DMAP (2.2 mg, 0.018 mmol) in DCM (5 mL). After 24 h of stirring, the solvent was evaporated and pure **7** (first fraction) was isolated by chromatography on silica gel (50 mL, *n*-hexane/ethyl acetate 3:2) as an orange solid (111 mg, 56.3%). ^{1}H NMR (600 MHz, $CDCl_3$): δ = 7.35–7.40 (m, 2H), 7.31–7.35 (m, 1H), 7.25–7.30 (m, 2H), 5.16 (d, J = 5.9 Hz, 1H), 5.13 (d, J = 5.9 Hz, 1H), 4.13 (s, 5H), 4.10 (s, 2H), 4.08 (s, 2H), 2.84–2.90 (m, 1H), 2.77–2.83 (m, 1H), 2.42 (t, J = 7.8 Hz, 2H), 1.86–1.96 (m, 2H), 0.82 (t, J = 8.0 Hz, 9H), 0.42–0.55 ppm (m, 6H); ^{13}C{^{1}H} NMR (151 MHz, $CDCl_3$): δ = 171.0, 166.6, 133.5, 128.3, 128.1, 127.9, 88.1, 77.0, 68.5, 68.2, 68.1, 67.3, 67.2, 61.0, 36.7, 28.9, 25.4, 6.2, 4.4 ppm; HRMS (EI) calculated for $C_{29}H_{37}FeNO_3Si$ 531.18872, found 531.18899.

2′,7-*O*-Bis(trietylsilyl)-*N*-debenzoyl-*N*-ferrocenoylpaclitaxel (**8**): 7-*O*-Triethylsilylbaccatin III (**4**, 352 mg, 0.503 mmol) and (3*R*,4*S*)-1-ferrocenoyl-4-phenyl-3-((triethylsilyl)oxy)azetidin-2-one (**6**, 430 mg, 0.879 mmol) in anhydrous THF (20 mL) were placed in a Schlenk tube. LiHMDS (1.0 M in THF, 0.820 mL, 0.820 mmol) was added at −40 °C and the resulting solution was stirred at this temperature for 40 min. The reaction was quenched by addition of 40 mL of saturated ammonium chloride and the product was extracted with ethyl acetate. The organic solution was washed with water, brine and the solvents were evaporated. The pure product was isolated by chromatography on silica gel (70 mL, *n*-hexane/ethyl acetate 2:1) as a yellow solid (445 mg, 74.5%). ^{1}H NMR (600 MHz, $CDCl_3$): δ = 8.16 (d, J = 7.6 Hz, 2H), 7.63 (t, J = 7.9 Hz, 1H), 7.55 (t, J = 7.7 Hz, 2H), 7.37–7.42 (m, 3H), 7.32 (t, J = 7.3 Hz, 1H), 6.70 (d, J = 8.9 Hz, 1H), 6.48 (s, 1H), 6.31 (t, J = 8.8 Hz, 1H), 5.73 (d, J = 7.1 Hz, 1H), 5.63 (d, J = 8.6 Hz, 1H), 4.96 (dd, J = 1.6, 7.9 Hz, 1H), 4.70 (d, J = 1.8 Hz, 1H), 4.66 (br s, 1H), 4.61 (br s, 1H), 4.50 (dd, J = 6.7, 10.6 Hz, 1H), 4.33 (br s, 3H), 4.23 (d, J = 8.4 Hz, 1H), 4.18 (s, 5H), 3.86 (d, J = 7.0 Hz, 1H), 2.53–2.57 (m, 1H), 2.52 (s, 3H), 2.44 (dd, J = 9.6, 15.2 Hz, 1H), 2.20–2.26 (m, 1H), 2.18 (s, 3H), 2.04 (d, J = 0.9 Hz, 3H), 1.92 (quint, J = 2.1, 10.7 Hz, 1H), 1.87 (br s, 1H), 1.72 (s, 3H), 1.23 (s, 3H), 1.20 (s, 3H), 0.94 (t, J = 7.9 Hz, 9H), 0.88 (t, J = 7.9 Hz, 9H), 0.57–0.65 (m, 6H), 0.51–0.57 (m, 3H), 0.44–0.51 ppm (m, 3H); ^{13}C{^{1}H} NMR (151 MHz, $CDCl_3$): δ = 201.7, 171.5, 170.0, 169.7, 169.3, 167.0, 140.2, 139.0, 133.8, 133.6 (CH), 130.3 (CH), 129.3, 128.8 (CH), 128.6 (CH), 127.9 (CH), 126.5 (CH), 84.2 (CH), 81.2, 78.8, 76.6 (CH_2), 75.7, 75.0 (CH), 75.0 (CH), 74.8 (CH), 72.2 (CH), 71.4 (CH), 70.6 (CH), 70.4 (CH), 69.8 (CH), 68.5 (CH), 67.9 (CH), 58.4, 55.1 (CH), 46.7 (CH), 43.4, 37.3 (CH_2), 35.7 (CH_2), 26.6 (CH), 23.0 (CH), 21.5 (CH), 20.8 (CH), 14.1 (CH), 10.1 (CH), 6.7 (CH), 6.5 (CH), 5.3 (CH_2), 4.5 ppm (CH_2); MALDI calculated for $C_{63}H_{83}FeNO_{14}Si_2$ 1189.47, found 1189.35.

***N*-Debenzoyl-*N*-ferrocenoylpaclitaxel** (**10**): A large excess of hydrogen fluoride·pyridine complex (3.7 mL) was added to a solution of **8** (445 mg, 0.374 mmol) in a mixture of anhydrous acetonitrile (15 mL) and anhydrous pyridine (30 mL) placed in a Teflon flask. The solution was stirred at RT for 20 h, the reaction was then quenched by addition of saturated sodium bicarbonate (400 mL) and the product was extracted with ethyl acetate. The organic

phase was washed with water, brine and the solvents were evaporated. The pure product (323 mg, 90%) was isolated by chromatography on silica gel (300 mL, dichloromethane/methanol 97:3). ^{1}H NMR (600 MHz, $CDCl_3$): δ = 8.15 (dd, J = 1.3, 7.2 Hz, 2H), 7.66–7.63 (m, 1H), 7.54 (t, J = 7.8 Hz, 2H), 7.50 (d, J = 7.4 Hz, 2H), 7.44 (t, J = 7.7 Hz, 2H), 7.36 (t, J = 7.4 Hz, 1H), 6.48 (d, J = 8.9 Hz, 1H), 6.30 (s, 1H), 6.28 (d, J = 9.0 Hz, 1H), 5.72 (dd, J = 2.5, 8.9 Hz, 1H), 5.70 (d, J = 7.0 Hz, 1H), 4.96 (dd, J = 2.0, 9.6 Hz, 1H), 4.78 (dd, J = 2.7, 5.1 Hz, 1H), 4.65–4.64 (m, 1H), 4.64–4.63 (m, 1H), 4.44–4.40 (m, 1H), 4.35 (t, J = 1.6 Hz, 2H), 4.31 (d, J = 8.5 Hz, 1H), 4.22 (d, J = 8.3 Hz, 1H), 4.16 (s, 5H), 3.82 (d, J = 7.0 Hz, 1H), 3.62 (d, J = 5.2 Hz, 1H), 2.56 (ddd, J = 5.3, 6.6, 6.8 Hz, 1H), 2.43 (d, J = 4.1 Hz, 1H), 2.39 (s, 3H), 2.35 (dd, J = 9.2, 12.2 Hz, 1H), 2.25 (s, 3H), 1.92–1.84 (m, 1H), 1.84 (d, J = 1.1 Hz, 1H), 1.70 (s, 3H), 1.33–1.28 (m, 1H), 1.27 (s, 3H), 1.16 ppm (s, 3H); ^{13}C{^{1}H} NMR (151 MHz, $CDCl_3$): δ = 203.6, 172.7, 171.2, 170.3, 167.0, 142.0, 138.5, 133.7 (CH), 133.2, 130.2 (CH), 129.2, 129.0 (CH), 128.8 (CH), 128.3 (CH), 127.1 (CH), 84.4 (CH), 81.2, 79.0, 77.2 (CH), 76.5 (CH_2), 75.6 (CH), 75.0 (CH), 73.4 (CH), 72.3 (CH), 72.2 (CH), 70.5 (CH), 69.0 (CH), 58.6, 54.6 (CH), 45.6 (CH), 43.2, 35.7 (CH_2), 35.6 (CH_2), 26.9 (CH), 22.7 (CH), 21.8 (CH), 20.8 (CH), 14.8 (CH), 9.6 ppm (CH). MALDI calculated for $C_{51}H_{55}FeNO_{14}$ 961.30, found 961.39.

2′-*O*-(4-Ferrocenylbutyryl)paclitaxel (**14**): This compound was synthesised in 64% yield (71 mg) as described previously,[20] starting from paclitaxel (**1**, 85 mg, 0.100 mmol), 4-ferrocenylbutyric acid (30 mg 0.110 mmol), DMAP (13 mg, 0.106 mmol) and DIC (25 mg, 31 μL, 0.200 mmol). ^{1}H NMR ($CDCl_3$, 600 MHz): δ = 8.15 (d, J = 7.5 Hz, 2H), 7.73 (brs, 2H), 7.58–7.65 (m, 1H), 7.53 (t, J = 7.6 Hz, 3H), 7.42 (brs, 4H), 7.36 (d, J = 6.5 Hz, 3H), 6.80 (brs, 1H), 6.32 (s, 1H), 6.27 (t, J = 8.8 Hz, 1H), 5.98 (brs, 1H), 5.70 (d, J = 7.1 Hz, 1H), 5.51 (brs, 1H), 4.99 (d, J = 8.4 Hz, 1H), 4.43–4.50 (m, 1H), 4.33 (dd, J = 1.0, 8.4 Hz, 1H), 4.53–4.11 (bs, 9H), 4.22 (d, J = 8.4 Hz, 1H), 3.84 (d, J = 7.0 Hz, 1H), 2.54–2.62 (m, 1H), 2.42–2.52 (m, 5H), 2.38 (dd, J = 9.3, 15.3 Hz, 1H), 2.23 (s, 3H), 2.10–2.20 (m, 1H), 1.96 (s, 3H), 1.86–1.93 (m, 1H), 1.75 (s, 2H), 1.70 (s, 3H), 1.61 (s, 3H), 1.25 (s, 3H), 1.15 ppm (s, 3H); ^{13}C{^{1}H} NMR (151 MHz, $CDCl_3$): δ = 203.8, 171.2, 169.8, 168.1, 167.1, 167.0, 142.8, 137.1, 133.8, 133.7 (CH), 132.8, 132.0 (CH), 130.2 (CH), 129.3, 129.1 (CH), 128.8 (CH), 128.8 (CH), 128.4 (CH), 127.2 (CH), 126.7 (CH), 84.5 (CH), 81.1, 79.3, 76.5 (CH_2), 75.6 (CH), 75.2 (CH), 74.0 (CH), 72.1 (CH), 71.8 (CH), 69.7 (bs, 3×CH, 2Cp), 58.6, 52.8 (CH), 45.6 (CH), 43.2, 35.6 (CH_2), 35.6 (CH_2), 33.8 (CH_2), 30.5 (CH_2), 29.4, 28.9 (CH_2), 26.9 (CH), 24.7, 22.8 (CH), 22.1 (CH), 20.8 (CH), 14.8 (CH), 9.6 ppm (CH); MALDI calculated for $C_{61}H_{65}FeNO_{15}$ 1107.37, found 1107.45.

2′-*O*-(4-Ferrocenylbutyryl)docetaxel (**18**): This compound was synthesised in 44% yield (47 mg) by the method described previously,[20] starting from docetaxel (**2**, 81 mg, 0.100 mmol), 4-ferrocenylbutyric acid (30 mg, 0.110 mmol), DMAP (13 mg, 0.106 mmol) and DIC (25 mg, 31 μL, 0.200 mmol). ^{1}H NMR (600 MHz, $CDCl_3$): δ = 8.13 (d, J = 7.5 Hz, 2H), 7.62 (t, J = 7.3 Hz, 1H), 7.51 (t, J = 7.7 Hz, 2H), 7.37–7.43 (m, 2H), 7.27–7.36 (m, 3H), 6.26 (brs, 1H), 5.70 (d, J = 7.2 Hz, 1H), 5.48 (brs, 1H), 5.39 (brs, 1H), 5.34 (m., 1H), 5.22 (s, 1H), 4.98 (d, J = 9.0 Hz, 1H), 4.33 (d, J = 8.3 Hz, 1H), 4.27 (brs, 9H), 4.21 (d, J = 8.7 Hz, 1H), 4.18 (s, 2H), 3.95 (d, J = 7.2 Hz, 1H), 2.56–2.64 (m, 1H), 2.37–2.48 (m, 4H) 2.34 (brs, 1H), 2.18 (brs, 2H), 1.97 (s, 3H), 1.86 (t, J = 12.2 Hz, 1H), 1.77 (s, 3H), 1.68–1.74 (m, 2H), 1.66 (s, 1H), 1.35 (s, 9H), 1.23–1.27 (m, 5H), 1.11–1.17 ppm (m, 3H); ^{13}C{^{1}H} NMR (151 MHz, $CDCl_3$): δ = 211.6, 172.5, 169.7, 168.1, 167.1, 139.2, 137.6, 135.6, 133.6 (CH), 130. (CH), 129.3, 128.9 (CH), 128.7 (CH), 128.1 (CH), 126.3 (CH), 84.2 (CH), 81.0, 80.4, 77.2 (CH), 79.0, 76.6 (CH_2), 75.1 (CH), 74.5 (CH), 74.2 (CH), 71.9 (CH), 71.9 (CH), 69.6 (CH), 69.0 (CH), 68.3 (CH), 57.6, 54.1, 46.4 (CH), 43.1, 37.0 (CH_2), 35.6 (CH_2), 33.2 (CH_2), 29.3, 28.6 (CH_2), 28.2 (CH), 26.4 (CH), 25.8 (CH_2), 22.6 (CH), 20.9 (CH), 14.2 (CH), 10.0 ppm (CH); MALDI calculated for $C_{57}H_{67}FeNO_{15}$ 1061.39, found 1061.40.

2′-*O*-(*tert*-Butyldimethylsilyl)-7-*O*-(3-ferrocenoylpropioyl)paclitaxel (**22**): DIC (21 mg, 26 μL, 0.165 mmol) was added to a solution of **20** (100 mg, 0.103 mmol), 3-ferrocenoylpropionic acid (44 mg, 0.155 mmol) and DMAP (5 mg, 0.041 mmol) in anhydrous dichloromethane (1 mL). The resulting solution was stirred at RT for 5 h and the solvent evaporated. The pure product was isolated by chromatography on silica gel (100 mL, *n*-hexane/ethyl acetate 2:1) as an orange solid (105 mg, 82%). ^{1}H NMR (600 MHz, $CDCl_3$): δ = 8.12–8.17 (m, 2H), 7.73–7.78 (m, 2H), 7.58–7.65 (m, 1H), 7.52–7.56 (m, 2H), 7.50 (td, J = 1.5, 7.5 Hz, 1H), 7.41–7.45 (m, 2H), 7.37–7.41 (m, 2H), 7.29–7.36 (m, 3H), 7.08 (d, J = 8.9 Hz, 1H), 6.31 (s, 1H), 6.24–6.30 (m, 1H), 5.75 (dd, J = 1.7, 8.9 Hz, 1H), 5.72 (d, J = 7.0 Hz, 1H), 5.67 (dd, J = 7.1, 10.6 Hz, 1H), 5.00 (d, J = 8.1 Hz, 1H), 4.82–4.87 (m, 2H), 4.69 (d, J = 2.1 Hz, 1H), 4.50 (t, J = 1.9 Hz, 2H), 4.34 (s, 1H), 4.25 (s, 5H), 4.23 (d, J = 8.7 Hz, 1H), 3.99 (d, J = 6.9 Hz, 1H), 3.15 (td, J = 7.5, 17.7 Hz, 1H), 3.00–3.08 (m, 1H), 2.62–2.78 (m, 3H), 2.58 (s, 3H), 2.44 (dd, J = 9.5, 15.2 Hz, 1H), 2.20 (s, 3H), 2.14–2.21 (m, 1H), 2.00 (d, J = 1.2 Hz, 3H), 1.93 (ddd, J = 2.0, 10.8, 14.5 Hz, 1H), 1.85 (s, 3H), 1.71 (s, 1H), 1.23 (s, 3H), 1.19 (s, 3H), 0.81 (s, 9H), −0.03 (s, 3H), −0.29 ppm (s, 3H); ^{13}C{^{1}H} NMR (151 MHz, $CDCl_3$): δ = 202.5, 202.0, 172.2, 171.5, 169.8, 169.0, 167.0, 167.0, 140.9, 138.3, 134.2, 133.7 (CH), 132.7, 131.8 (CH), 130.2 (CH), 129.2, 128.8 (CH), 128.7 (CH), 128.0 (CH), 127.0 (CH), 126.4 (CH), 84.1 (CH), 81.1, 78.7, 78.7, 76.4 (CH_2), 75.4 (CH), 75.1 (CH), 74.6 (CH), 72.1 (CH), 72.1 (CH), 71.3 (CH), 69.9 (CH), 69.3 (CH), 69.3 (CH), 56.2, 55.7 (CH), 47.0 (CH), 43.4, 35.6 (CH_2), 34.3 (CH_2), 33.4 (CH_2), 28.3 (CH_2), 26.4 (CH), 25.5 (CH), 23.0 (CH), 21.4 (CH), 20.8 (CH), 18.1, 14.6 (CH), 14.2, 10.9 (CH), −5.2 (CH), −5.8 ppm; MALDI calculated for $C_{67}H_{77}FeNO_{16}Si$ 1235.44, found 1235.35.

Acknowledgements

This work was financially supported by the National Science Centre Poland (NCN) based on the decision DEC-2012/05/B/ST5/00300.

Keywords: bioorganometallic chemistry · cancer · medicinal chemistry · microtubule · tubulin polymerisation

[1] M. C. Wani, H. L. Taylor, M. E. Wall, P. Coggon, A. T. McPhail, *J. Am. Chem. Soc.* **1971**, *93*, 2325–2327.

[2] a) P. B. Schiff, J. Fant, S. B. Horwitz, *Nature* **1979**, *277*, 665–667; b) M. A. Jordan, *Curr. Med. Chem. Anti-Cancer Agents* **2002**, *2*, 1–17.

[3] M. L. Miller, I. Ojima, *Chem. Rec.* **2001**, *1*, 195–211.

[4] M. Rooseboom, J. N. Commandeur, N. P. Vermeulen, *Pharmacol. Rev.* **2004**, *56*, 53–102.

[5] E. K. Rowinsky, *Annu. Rev. Med.* **1997**, *48*, 353–374.

[6] a) I. Ojima, J. C. Slater, E. Michaud, S. D. Kuduk, P.-Y. Bounaud, P. Vrignaud, M.-C. Bissery, J. M. Veith, P. Pera, R. J. Bernacki, *J. Med. Chem.* **1996**, *39*, 3889–3896; b) S. M. Ali, M. Z. Hoemann, J. Aubé, G. I. Georg, L. A. Mitscher, L. R. Jayasinghe, *J. Med. Chem.* **1997**, *40*, 236–241; c) D. G. I. Kingston, A. G. Chaudhary, M. D. Chordia, M. Gharpure, A. A. L. Gunatilaka, P. I. Higgs, J. M. Rimoldi, L. Samala, P. G. Jagtap, P. Giannakakou, Y. Q. Jiang, C. M. Lin, E. Hamel, B. H. Long, C. R. Fairchild, K. A. Johnston, *J. Med. Chem.* **1998**, *41*, 3715–3726; d) T. J. Altstadt, C. R. Fairchild, J. Golik, K. A. Johnston, J. F. Kadow, F. Y. Lee, B. H. Long, W. C. Rose, D. M. Vyas, H. Wong, M.-J. Wu, M. D. Wittman, *J. Med. Chem.* **2001**, *44*, 4577–4583; e) I. Ojima, C. P. Borella, X. Wu, P.-Y. Bounaud, C. F. Oderda, M. Sturm, M. L. Miller, S. Chakravarty, J. Chen, Q. Huang, P. Pera, T. A. Brooks, M. R. Baer, R. J. Bernacki, *J. Med. Chem.* **2005**, *48*, 2218–2228; f) I. Ojima, J. Chen, L. Sun, C. P. Borella, T. Wang, M. L. Miller, S. Lin, X. Geng, L. Kuznetsova, C. Qu, D. Gallager, X. Zhao, I. Zanardi, S. Xia, S. B.

Horwitz, J. Mallen-St. Clair, J. L. Guerriero, D. Bar-Sagi, J. M. Veith, P. Pera, R. J. Bernacki, *J. Med. Chem.* **2008**, *51*, 3203 – 3221; g) L. V. Kuznetsova, A. Pepe, I. M. Ungureanu, P. Pera, R. J. Bernacki, I. Ojima, *J. Fluorine Chem.* **2008**, *129*, 817 – 828; h) M. Hidaka, T. Koga, H. Kiyota, T. Horiguchi, Q.-W. Shi, K. Hirose, T. Uchida, *Biosci., Biotechnol., Biochem.* **2012**, *76*, 349 – 352; i) A. R. Wohl, A. R. Michel, S. Kalscheuer, C. W. Macosko, J. Panyam, T. R. Hoye, *J. Med. Chem.* **2014**, *57*, 2368 – 2379; j) R. Matesanz, C. Trigili, J. Rodríguez-Salarichs, I. Zanardi, B. Pera, A. Nogales, W. S. Fang, J. Jímenez-Barbero, Á. Canales, I. Barasoain, I. Ojima, J. F. Díaz, *Bioorg. Med. Chem.* **2014**, *22*, 5078 – 5090.

[7] a) E. J. Roh, C. E. Song, D. Kim, H. O. Pae, H. T. Chung, K. S. Lee, K. B. Chai, C. O. Lee, S. U. Choi, *Bioorg. Med. Chem.* **1999**, *7*, 2115 – 2119; b) E. J. Roh, D. Kim, C. O. Lee, S. U. Choi, C. E. Song, *Bioorg. Med. Chem.* **2002**, *10*, 3145 – 3151.

[8] L. Kuznetsova, J. Chen, L. Sun, X. Wu, A. Pepe, J. M. Veith, P. Pera, R. J. Bernacki, I. Ojima, *Bioorg. Med. Chem. Lett.* **2006**, *16*, 974 – 977.

[9] O. N. Zefirova, E. V. Nurieva, A. N. Ryzhov, N. V. Zyk, N. S. Zefirov, *Russ. J. Org. Chem.* **2005**, *41*, 315 – 351.

[10] a) M. F. R. Fouda, M. M. Abd-Elzaher, R. A. Abdelsamaia, A. A. Labib, *Appl. Organomet. Chem.* **2007**, *21*, 613 – 625; b) E. Meléndez, *Inorg. Chim. Acta* **2012**, *393*, 36 – 52; c) S. S. Braga, A. M. S. Silva, *Organometallics* **2013**, *32*, 5626 – 5639; d) S. Moon, M. Hanif, M. Kubanik, H. Holtkamp, T. Söhnel, S. M. F. Jamieson, C. G. Hartinger, *ChemPlusChem* **2015**, *80*, 231 – 236.

[11] a) C. Biot, F. Nosten, L. Fraisse, D. Ter-Minassian, J. Khalife, D. Dive, *Parasite* **2011**, *18*, 207 – 214; b) W. A. Wani, E. Jameel, U. Baig, S. Mumtazuddin, L. T. Hun, *Eur. J. Med. Chem.* **2015**, *101*, 534 – 551.

[12] a) M. Wenzel, M. Patra, C. H. R. Senges, I. Ott, J. J. Stepanek, A. Pinto, P. Prochnow, C. Vuong, S. Langklotz, N. Metzler-Nolte, J. E. Bandow, *ACS Chem. Biol.* **2013**, *8*, 1442 – 1450; b) Y. Liu, H. Zhang, D. Yin, D. Chen, *Res. Chem. Intermed.* **2015**, *41*, 3793—3801; c) S. Mishra, V. Tirkey, A. Ghosh, H. R. Dash, S. Das, M. Shukla, S. Saha, S. M. Mobin, S. Chatterjee, *J. Mol. Struct.* **2015**, *1085*, 162 – 172.

[13] a) P. Meunier, I. Ouattara, B. Gautheron, J. Tirouflet, D. Camboli, J. Besançon, *Eur. J. Med. Chem.* **1991**, *26*, 351 – 362; b) A. A. Simenel, G. A. Dokuchaeva, L. V. Snegur, A. N. Rodionov, M. M. Ilyin, S. I. Zykova, L. A. Ostrovskaya, N. V. Bluchterova, M. M. Fomina, V. A. Rikova, *Appl. Organomet. Chem.* **2011**, *25*, 70 – 75; c) K. Kowalski, A. Koceva-Chyła, A. Pieniążek, J. Bernasińska, J. Skiba, A. J. Rybarczyk-Pirek, Z. Jóźwiak, *J. Organomet. Chem.* **2012**, *700*, 58 – 68.

[14] B. Long, S. Liang, D. Xin, Y. Yang, J. Xiang, *Eur. J. Med. Chem.* **2009**, *44*, 2572 – 2576.

[15] a) D. Plażuk, A. Vessières, E. A. Hillard, O. Buriez, E. Labbé, P. Pigeon, M.-A. Plamont, C. Amatore, J. Zakrzewski, G. Jaouen, *J. Med. Chem.* **2009**, *52*, 4964 – 4967; b) E. Hillard, A. Vessières, G. Jaouen in *Medicinal Organometallic Chemistry, Vol. 32* (Eds.: G. Jaouen, N. Metzler-Nolte), Springer, Berlin Heidelberg, **2010**, pp. 81 – 117.

[16] a) S. Top, J. Tang, A. Vessieres, D. Carrez, C. Provot, G. Jaouen, *Chem. Commun.* **1996**, 955 – 956; b) S. Top, B. Dauer, J. Vaissermann, G. Jaouen, *J. Organomet. Chem.* **1997**, *541*, 355 – 361; c) E. Hillard, A. Vessieres, F. Le Bideau, D. Plazuk, D. Spera, M. Huche, G. Jaouen, *ChemMedChem* **2006**, *1*, 551 – 559; d) N. Chavain, C. Biot, *Curr. Med. Chem.* **2010**, *17*, 2729 – 2745; e) G. Gasser, I. Ott, N. Metzler-Nolte, *J. Med. Chem.* **2011**, *54*, 3 – 25; f) D. Plażuk, S. Top, A. Vessières, M.-A. Plamont, M. Huché, J. Zakrzewski, A. Makal, K. Woźniak, G. Jaouen, *Dalton Trans.* **2010**, *39*, 7444 – 7450; g) D. Plażuk, B. Rychlik, A. Błauż, S. Domagała, *J. Organomet. Chem.* **2012**, *715*, 102 – 112; h) G. Gasser, N. Metzler-Nolte, *Curr. Opin. Chem. Biol.* **2012**, *16*, 84 – 91; i) A. Vessières, *J. Organomet. Chem.* **2013**, *734*, 3 – 16.

[17] a) C. Biot, W. Daher, C. M. Ndiaye, P. Melnyk, B. Pradines, N. Chavain, A. Pellet, L. Fraisse, L. Pelinski, C. Jarry, J. Brocard, J. Khalife, I. Forfar-Bares, D. Dive, *J. Med. Chem.* **2006**, *49*, 4707 – 4714; b) F. Dubar, G. Anquetin, B. Pradines, D. Dive, J. Khalife, C. Biot, *J. Med. Chem.* **2009**, *52*, 7954 – 7957.

[18] a) M. Patra, K. Ingram, V. Pierroz, S. Ferrari, B. Spingler, J. Keiser, G. Gasser, *J. Med. Chem.* **2012**, *55*, 8790 – 8798; b) E. M. Lewandowski, J. Skiba, N. J. Torelli, A. Rajnisz, J. Solecka, K. Kowalski, Y. Chen, *Chem. Commun.* **2015**, *51*, 6186 – 6189.

[19] A. Arezki, G. G. Chabot, L. Quentin, D. Scherman, G. Jaouen, E. Brulé, *MedChemComm* **2011**, *2*, 190 – 195.

[20] D. Plażuk, A. Wieczorek, A. Błauż, B. Rychlik, *MedChemComm* **2012**, *3*, 498 – 501.

[21] A. Wieczorek, A. Błauż, J. Zakrzewski, B. Rychlik, D. Plażuk, *ACS Med. Chem. Lett.* **2016**, *7*, 612 – 617.

[22] a) G. I. Georg, G. C. B. Harriman, M. Hepperle, J. S. Clowers, D. G. Vander Velde, R. H. Himes, *J. Org. Chem.* **1996**, *61*, 2664 – 2676; b) I. Ojima, S. D. Kuduk, S. Chakravarty in *Advances in Medicinal Chemistry, Vol. 4* (Eds.: E. M. Bruce, B. R. Allen), Elsevier, **1999**, 69 – 124; c) I. Ojima, S. Lin, T. Inoue, M. L. Miller, C. P. Borella, X. Geng, J. J. Walsh, *J. Am. Chem. Soc.* **2000**, *122*, 5343 – 5353.

[23] I. Paterson, G. J. Naylor, T. Fujita, E. Guzman, A. E. Wright, *Chem. Commun.* **2010**, *46*, 261 – 263.

[24] N. M. Saied, N. Mejri, R. E. Aissi, E. Benoist, M. Saidi, *Eur. J. Med. Chem.* **2015**, *97*, 280 – 288.

[25] a) N. F. Magri, D. G. I. Kingston, *J. Nat. Prod.* **1988**, *51*, 298 – 306; b) B. J. Turunen, H. Ge, J. Oyetunji, K. E. Desino, V. Vasandani, S. Güthe, R. H. Himes, K. L. Audus, A. Seelig, G. I. Georg, *Bioorg. Med. Chem. Lett.* **2008**, *18*, 5971 – 5974; c) P. Wender, E. A. Dubikovskaya, S. H. Thorne, C. H. Contag, Leland Stanford Junior University, USA, **2009**, WO2009099636 A1d) D. M. Nevarez, Y. A. Mengistu, I. N. Nawarathne, K. D. Walker, *J. Am. Chem. Soc.* **2009**, *131*, 5994 – 6002.

[26] B. Rychlik, Ł. Pułaski, Ł. Piotrowski, P. Guzenda, E. Macierzyńska, A. Grzelak, G. Bartosz, *FEBS Special Meeting ATP-Binding Cassette (ABC) Proteins: From Multidrug Resistance to Genetic Diseases*, Innsbruck, Austria, March 4 – 10, **2006**.

[27] P. Wils, V. Phung-Ba, A. Warnery, D. Lechardeur, S. Raeissi, I. J. Hidalgo, D. Scherman, *Biochem. Pharmacol. (Amsterdam, Neth.)* **1994**, *48*, 1528 – 1530.

[28] Taxol injection label on FDA homepage, reference ID: 2939751 (http://www.accessdata.fda.gov/drugsatfda docs/label/2011/020262s049Lbl.pdf).

[29] A. Błauż, B. Rychlik unpublished results.

[30] G. Jones, P. Willett, R. C. Glen, A. R. Leach, R. Taylor, *J. Mol. Biol.* **1997**, *267*, 727 – 748.

[31] a) G. Jaouen, S. Top in *Advances in Organometallic Chemistry and Catalysis: The Silver/Gold Jubilee International Conference on Organometallic Chemistry Celebratory Books* (Ed.: A. J. L. Pombeiro), John Wiley & Sons, Inc., Hoboken **2013**, pp. 563 – 580; b) H. Z. S. Lee, O. Buriez, F. Chau, E. Labbé, R. Ganguly, C. Amatore, G. Jaouen, A. Vessières, W. K. Leong, S. Top, *Eur. J. Inorg. Chem.* **2015**, 4217 – 4226.

[32] J. Keiser, M. Vargas, R. Rubbiani, G. Gasser, C. Biot, *Parasites Vectors* **2014**, *7*, 424.

[33] R. Rubbiani, O. Blacque, G. Gasser, *Dalton Trans.* **2016**, *45*, 6619 – 6626.

Received: April 18, 2016
Published online on July 4, 2016